Thermochemistry of Fluorinated Single Wall Carbon Nanotubes

Holger F. Bettinger,*,† Konstantin N. Kudin, and Gustavo E. Scuseria

Contribution from the Department of Chemistry, MS-60, and Center for Nanoscale Science and Technology, Rice University, P.O. Box 1892, Houston, Texas 77251-1892

Received April 16, 2001

Abstract: The gradient corrected Perdew−Burke−Ernzerhof density functional in conjunction with a 3-21G basis set and periodic boundary conditions was employed to investigate the geometries and energies of C_2F fluorinated armchair single wall carbon nanotubes (F−SWNT's) with diameters ranging from 16.4 to 4.2 Å [(12,12) to (3,3)] as well as a C_2F graphene sheet fluorinated on one side only. Using an isodesmic equation, we find that the thermodynamic stability of F−SWNT's increases with decreasing tube diameter. On the other hand, the mean bond dissociation energies of the C−F bonds increase as the tubes become thinner. The C−F bonds in the (5,5) F−SWNT's are about as strong as those in graphite fluoride $(CF)_n$ and are also covalent albeit slightly (<0.04 Å) stretched. Whereas a fluorine atom is found not to bind covalently to the concave surface of [60]fullerene, endohedral covalent binding is possible inside a (5,5) SWNT despite a diameter similar to that of the C_{60} cage.

I. Introduction

The 1991 discovery of multiwall carbon nanotubes (CNT's) by Iijima[1] initiated an enormous activity in the investigation of synthesis and properties of these new tubular forms of carbon. As discussed in detail in several monographs,[2−4] CNT's are comprised of a rolled graphite sheet ("graphene") and closed by fullerene-like caps. Depending on the way the graphene is rolled, different chiralities are possible, which are commonly distinguished by their chiral vector (*n*,*m*). The (*n*,*n*) tubes are called "armchair" and the (*n*,0) are called "zigzag" nanotubes. A simple analysis imposing appropriate boundary conditions on the graphene band structure[5] predicts that the armchair tubes are metallic (i.e., the band gap is zero due to band crossing), whereas the zigzag tubes are either semimetals or semiconductors, depending on the value of *n*.[6] The computations of the band structures using density functional theory (plane-wave pseudopotential local density approximation) indicate that these simple rules need to be refined, at least for narrow zigzag tubes.[7] It was found by these calculations that the rehybridization of the carbon states due to the strong curvature of small tubes introduces low-lying conduction band states into the band gap of insulating tubes.[7]

Whereas Iijima's multiwall CNT's consist of at least two concentric tubes, single wall carbon nanotubes (SWNT's) are produced by laser vaporization of a metal−graphite (Co, Ni) target.[8,9] These SWNT's are comprised of a single rolled graphene sheet but have a tendency to form "ropes", i.e., bundles of SWNT's. The tubes produced by the laser-oven technique have very uniform diameter around 1.38 ± 0.02 nm, according to X-ray diffraction, and an intertube distance of 0.315 nm in the ropes, similar to that in crystalline C_{60}. It was concluded that the ropes are made up primarily of (10,10) armchair SWNT's.[9]

The rolling of the graphene sheet induces strain, but for large-diameter SWNT's the strain energy per carbon atom, E_s, is small. It was shown that $E_s \propto D^{-2}$, where D is the tube diameter.[10,11] Consequently, the chemistry of wide carbon nanotubes should be similar to that of graphite, whereas the narrower tubes are expected to be more reactive due to the larger strain of the carbon framework. Since the endcaps of nanotubes resemble fullerenes, whose five-membered rings are mainly responsible for their broad chemistry,[12] these are expected to be the most reactive part of any capped nanotube.

Indeed, it was shown that the end caps of nanotubes can be etched by acids and by ozone yielding nanotubes with functionalized end groups.[13−15] The controlled functionalization of nanotube side walls is more difficult to achieve. Chen et al. reported that treatment of end-carboxylated SWNT's with thionyl chloride and amines with long aliphatic tails yields

* To whom correspondence should be addressed.

† Present address: Lehrstuhl für Organische Chemie II, Ruhr-Universität Bochum, Universitätsstrasse 150, 44780 Bochum, Germany.

(1) Iijima, S. *Nature (London)* **1991**, *354*, 56.

(2) Dresselhaus, M. S.; Dresselhaus, G.; Eklund, P. C. *Science of Fullerenes and Carbon Nanotubes*; Academic Press: New York, 1996.

(3) *Carbon Nanotubes*; Ebbesen, T. W., Ed.; CRC Press: Boca Raton, FL, 1997.

(4) Harris, P. J. F. *Carbon Nanotubes and Related Structures*; Cambridge University Press: Cambridge, U.K., 1999.

(5) Wallace, P. R. *Phys. Rev.* **1947**, *71*, 622.

(6) Saito, R.; Fujita, M.; Dresselhaus, G.; Dresselhaus, M. S. *Phys. Rev. B* **1992**, *46*, 1804.

(7) Blase, X.; Benedict, L. X.; Shirley, E. L.; Louie, S. G. *Phys. Rev. Lett.* **1994**, *72*, 1878.

(8) Guo, T.; Nikolaev, P.; Thess, A.; Colbert, D. T.; Smalley, R. E. *Chem. Phys. Lett.* **1995**, *243*, 49.

(9) Thess, A.; Lee, R.; Nikolaev, P.; Dai, H. J.; Petit, P.; Robert, J.; Xu, C. H.; Lee, Y. H.; Kim, S. G.; Rinzler, A. G.; Colbert, D. T.; Scuseria, G. E.; Tománek, D.; Fischer, J. E.; Smalley, R. E. *Science* **1996**, *273*, 483.

(10) Mintmire, J. W.; White, C. T. In *Carbon Nanotubes*; Ebbesen, T. W., Ed.; CRC Press: Boca Raton, FL, 1997.

(11) Hernández, E.; Goze, C.; Bernier, P.; Rubio, A. *Appl. Phys. A* **1999**, *68*, 287.

(12) Hirsch, A. *The Chemistry of Fullerenes*; Georg Thieme Verlag: Stuttgart, Germany, 1994.

(13) Mawhinney, D. B.; Naumenko, V.; Kuznetsova, A.; Yates, J. T.; Liu, J.; Smalley, R. E. *J. Am. Chem. Soc.* **2000**, *122*, 2383.

(14) Liu, J.; Rinzler, A. G.; Dai, H. J.; Hafner, J. H.; Bradley, R. K.; Boul, P. J.; Lu, A.; Iverson, T.; Shelimov, K.; Huffman, C. B.; Rodriguez-Macias, F.; Shon, Y.-S.; Lee, T. R.; Colbert, D. T.; Smalley, R. E. *Science* **1998**, *280*, 1253.

(15) Sloan, J.; Hammer, J.; Zwiefka-Sibley, M.; Green, M. L. H. *Chem. Commun.* **1998**, 347.

10.1021/ja010977j CCC: $20.00
Published on Web 12/19/2001

SWNT's which are soluble in organic solvents.[16] These SWNT's can be derivatized using phenyl(bromodichloromethyl)mercury, a dichlorocarbene precursor.[17] However, due to large amounts of impurities in the SWNT sample (graphitic material and residual catalyst from the nanotube synthesis), it could not be proven beyond doubt that dichlorocarbene added to the SWNT side walls. Using density functional computations (up to the B3LYP/6-31G*//B3LYP/STO-3G level of theory) for nanotube models based on curved polycyclic aromatic hydrocarbons, Jaffe found that the binding energy of CC_{l2} to a nanotube side wall is small (−15 to −5 kcal mol^{-1}) and concluded that it is probably not possible to covalently add CCl_2 to SWNT's.[18]

Recently, Mickelson et al. reported that the fluorination of SWNT's is possible under conditions similar to those used for the fluorination of graphite.[19] If the reaction is performed at 325 °C, the fluorination is nondestructive and tubes with overall stoichiometry of approximately C_2F are obtained, whereas at 500 °C the tubes are destroyed.[19] Thus, C_2F appears to be the limiting stoichiometry for fluorination. Scanning tunneling microscopy (STM) shows that the side walls of SWNT's are covered with fluorine, although the cover is not distributed equally on the SWNT surface as narrow unfluorinated domains are recognizable.[20] Since the fluorinated SWNT's (F−SWNT's) are well soluble in organic solvents,[21] the F−SWNT's are useful precursors for further side wall derivatization.[22] For example, their reaction with Grignard or organolithium reagents yields SWNT carrying alkyl groups.[22] The reaction of F−SWNT's with anhydrous hydrazine allows to regenerate the unfluorinated, bare SWNT's.[19]

The fluorination of multiwall carbon nanotubes with elemental fluorine between room temperature (RT) and 500 °C produces fluorinated nanotubes of various composition, as Nakajima et al. demonstrated.[23] The fluorine content gets lower with increasing reaction temperature (C_4F at RT and $C_{16}F$ at 400 °C), but graphite fluoride $(CF)_x$ is formed at 500 °C, indicating that the tubes are opened under these conditions. According to infrared (IR) and X-ray photoelectron spectroscopy (XPS), the nature of the C−F bond changes from semicovalent to covalent with increasing temperatures.[23] The term "semicovalent" or "semiionic" C−F bonds is very often found in the literature of fluorine−graphite intercalation compounds (F−GIC's).[24] It is used to describe a C−F chemical bond with (primarily XPS) spectroscopic properties between those of ionic and covalent bonds of fluorine to the graphitic matrix.[25] The nature of the C−F bond in F−GIC's depends on the fluorine concentration and on the reaction conditions, and a thermodynamic analysis of the factors influencing the nature of the C−F bond in F-GIC's has been given by Dresselhaus et al.[26,27] Covalent attachment of fluorine to carbon was found by several groups who studied the fluorination of tubular carbon materials and characterized it using various analytical tools.[28−32]

Chart 1. Schematic Representation of a Graphene Sheet Covered to 50% by Fluorine Atoms (Black Dots) Resulting in Conjugated π Bond and Fluorine Atom Chains[a]

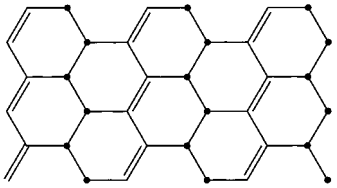

[a] Note that in the optimized structure (C_2F-**1**, PBC−PBE/3-21G, this work), the π bonds do not alternate and that the sheet is corrugated. Rolling this sheet into a (10,10) tube with π bond chains parallel to the tube axis, C_2F-**2**, produced the most stable all-outside F−SWNT studied by Kudin et al.[33]

To gain insight into the stability and properties of the fluorinated single wall carbon nanotubes synthesized at Rice University, we have very recently investigated the energies and band structures of the (10,10) and (18,0) C_2F F−SWNT's using density functional theory and periodic boundary conditions (PBC's).[33] The PBC approach allows the exploitation of translational symmetry and treats the system as an infinite polymer.[34] Earlier, Seifert et al. studied (10,0) C_2F and C_5F_2 F−SWNT's of various fluorination patterns employing a density functional based tight-binding approximation.[35] Among others, we investigated the F−SWNT's obtained by rolling a single sheet of graphite with a fluorine cover on one side, C_2F-**1**, as depicted in Chart 1. This sheet can be considered as being comprised of zigzag conjugated C−C π bonds and zigzag rows of fluorinated carbon atoms. Depending on the way this sheet is rolled, either armchair or zigzag F−SWNT's are formed with characteristic angles α between the π bond chains and the axis of the nanotube. We find that the (10,10) F−SWNT with $\alpha = 0°$ is metallic and the most stable isomer. All other (10,10) and (18,0) F−SWNT's isomers investigated, including those with isolated C═C bonds and cisoid rather than zigzag π bond chains, are less stable and have band gaps between 0.2 and 2.7 eV. These latter isomers are thus semiconducting or insulating depending on the way the fluorine atoms cover the SWNT surface.[33,35] In addition, we identified an even more stable structure with $\alpha = 0°$ by moving 50% of the fluorine atoms from the outside to the inside of the (10,10) SWNT in such a way as to preserve the conjugated π bond chains.[33]

(16) Chen, J.; Hamon, M. A.; Hu, H.; Chen, Y. S.; Rao, A. M.; Eklund, P. C.; Haddon, R. C. *Science* **1998**, *282*, 95.
(17) Chen, Y.; Haddon, R. C.; Fang, S.; Rao, A. M.; Lee, W. H.; Dickey, E. C.; Grulke, E. A.; Pendergrass, J. C.; Chavan, A.; Haley, B. E.; Smalley, R. E. *J. Mater. Res.* **1998**, *13*, 2423.
(18) Jaffe, R. L. *Proc.−Electrochem. Soc.* **1999**, *12*, 153.
(19) Mickelson, E. T.; Huffman, C. B.; Rinzler, A. G.; Smalley, R. E.; Hauge, R. H.; Margrave, J. L. *Chem. Phys. Lett.* **1998**, *296*, 188.
(20) Kelly, K. F.; Chiang, I. W.; Mickelson, E. T.; Hauge, R. H.; Margrave, J. L.; Wang, X.; Scuseria, G. E.; Radloff, C.; Halas, N. J. *Chem. Phys. Lett.* **1999**, *313*, 445.
(21) Mickelson, E. T.; Chiang, I. W.; Zimmerman, J. L.; Boul, P. J.; Lozano, J.; Liu, J.; Smalley, R. E.; Hauge, R. H.; Margrave, J. L. *J. Phys. Chem. B* **1999**, *103*, 4318.
(22) Boul, P. J.; Liu, J.; Mickelson, E. T.; Huffman, C. B.; Ericson, L. M.; Chiang, I. W.; Smith, K. A.; Colbert, D. T.; Hauge, R. H.; Margrave, J. L.; Smalley, R. E. *Chem. Phys. Lett.* **1999**, *310*, 367.
(23) Nakajima, T.; Kasamatsu, S.; Matsuo, Y. *Eur. J. Solid State Inorg. Chem.* **1996**, *33*, 831.
(24) *Fluorine-Carbon and Fluoride-Carbon Materials*; Nakajima, T., Ed.; Dekker: New York, 1995.
(25) Nakajima, T. In *Fluorine-Carbon and Fluoride-Carbon Materials*; Nakajima, T., Ed.; Dekker: New York, 1995; p 1.
(26) di Vittorio, S. L.; Dresselhaus, M. S.; Dresselhaus, G. *J. Mater. Res.* **1993**, *8*, 1578.
(27) Dresselhaus, M. S.; Endo, M.; Issi, J.-P. In *Fluorine-Carbon and Fluoride-Carbon Materials*; Nakajima, T., Ed.; Dekker: New York, 1995; p 95.
(28) Hamwi, A.; Alvergnat, H.; Bonnamy, S.; Béguin, F. *Carbon* **1997**, *35*, 723.
(29) Hattori, Y.; Watanabe, Y.; Kawasaki, S.; Okino, F.; Pradhan, B. K.; Kyotani, T.; Tomita, A.; Touhara, H. *Carbon* **1999**, *37*, 1033.
(30) Okotrub, A. V.; Yudanov, N. F.; Chuvilin, A. L.; Asanov, I. P.; Shubin, Y. V.; Bulusheva, L. G.; Gusel'nikov, A. V.; Fyodorov, I. S. *Chem. Phys. Lett.* **2000**, *322*, 231.
(31) Yudanov, N. F.; Okotrub, A. V.; Bulusheva, L. G.; Chuvilin, A. L.; Romanenko, A. I.; Asanov, I. P.; Shubin, Y. V.; Yudanova, L. I.; Fedorov, I. S. *Russ. J. Inorg. Chem.* **2000**, *45*, 1809.
(32) Touhara, H.; Okino, F. *Carbon* **2000**, *38*, 241.
(33) Kudin, K. N.; Bettinger, H. F.; Scuseria, G. E. *Phys. Rev. B* **2001**, *63*, 045413.
(34) Hoffmann, R. *Solids and Surfaces*; Wiley-VCH: New York, 1988.
(35) Seifert, G.; Köhler, T.; Frauenheim, T. *Appl. Phys. Lett.* **2000**, *77*, 1313.

Bauschlicher[38] recently studied the addition of fluorine atoms to a (10,0) SWNT using Morokuma's[36,37] ONIOM ("our own n-layered integrated molecular orbital and molecular mechanics") approach with a coronene-type ($C_{24}H_{12}$) high-level (B3LYP/6-31G*) area. A basic conclusion from Bauschlicher's work is that fluorine atoms tend to bind close to each other on the nanotube surface. However, the high-level model used was too small to predict the most favorable addition pattern on the zigzag tube.[33]

We here concentrate on the fluorination pattern with chains of fluorine atoms parallel to the nanotube axis, (*n*,*n*)-**2**, as this was identified in our earlier report to be the most favorable fluorine atom arrangement on C_2F armchair tubes.[33] We limit ourselves to the investigation of fluorinated armchair SWNT's, but investigate the stability of the F−SWNT's depending on the tube diameter. The strength and the nature of the C−F bonds in F−SWNT's receive particular attention.

II. Computational Methods

The computations reported here were performed using the gradient corrected density functional of Perdew, Burke, and Ernzerhof[39,40] (PBE) and Becke's[41] three-parameter hybrid functional in conjunction with the exchange-correlation functional of Lee, Yang, and Parr[42] (B3LYP). The computations were performed either on molecules or nanotube models of finite size (i.e., cluster approach) or on infinite systems by exploiting translational symmetry and imposing periodic boundary conditions (PBC's).[43] The nanotube clusters were terminated by hydrogen atoms to avoid polyradical character arising from dangling bonds. Both approaches use the 3-21G and 6-31G* Gaussian-type basis sets. The PBC computations were performed using the PBE functional (this level of theory is abbreviated as PBC−PBE throughout this paper). As described in detail elsewhere,[43−46] our new PBC implementation evaluates Coulomb interactions to infinity by using fast multipole methods within an accuracy of 10^{-9} atomic units. We used up to 128 **k** points for sampling the first Brillouin zone. In two-dimensional structures, graphene and C_2F-**1** sheets, a mesh of **k** points was employed with 128 points along the shorter translational vector and the proportionally smaller number along the longer vector. The first derivatives can be computed analytically and with a recently developed redundant internal coordinate method,[47] the optimization of geometries under periodic boundary conditions is efficient and straightforward. Geometries were completely optimized using the standard integration grid (75 radial shells and 302 angular points per shell), and the standard cutoffs of the Gaussian program.[48] All computations were performed with a development version of the Gaussian program.[48]

III. Results and Discussion

A. Thermodynamic Stability of Carbon Nanotubes. Previous computational studies found that carbon nanotubes are less stable than an infinite graphene sheet. This energy difference per carbon atom, called strain energy E_s of carbon nanotubes, arises from the curvature of the tube. In agreement with previous investigations,[10,11] we find at the PBC−PBE/3-21G level of theory that E_s is approximately proportional to D^{-2}, where D is the tube diameter (Figure 1). The strain energies obtained from our computations (Table 1) are similar to those obtained by Hernández et al. using the nonorthogonal tight-binding scheme.[11] The C−C bond distance in a graphene sheet is 1.431 Å at the PBC−PBE/3-21G level of theory, but the C−C bonds in the SWNT's studied here lengthen with decreasing tube diameter (Table 1). Note that the C−C bonds (R1) perpendicular to the tube axis are found to be slightly longer than the bonds R2 (Chart 2).

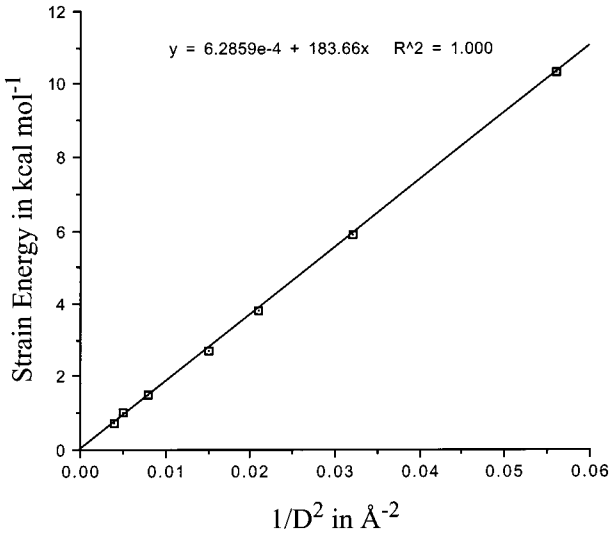

Figure 1. Plot of the strain energy per carbon atom (kcal mol^{-1}) in single wall carbon nanotubes (SWNT's) vs $1/D^2$ (D: diameter of SWNT). Data were obtained at the PBC−PBE/3-21G level of theory.

Table 1. Diameters (D, Å) and Strain Energies (E_s, kcal mol^{-1}) of (*n*,*n*) Armchair Single Wall Carbon Nanotubes Obtained at the PBC−PBE/3-21G Level of Theory

n	*D*/Å	R1	R2	E_s/(kcal mol^{-1})
3	4.235	1.449	1.441	10.3
4	5.572	1.442	1.436	5.9
5	6.920	1.438	1.435	3.8
6	8.272	1.436	1.434	2.7
7	9.632	1.435	1.433	1.9
8	10.991	1.434	1.433	1.5
9	12.351	1.434	1.433	1.2
10	13.714	1.433	1.432	1.0
12	16.440	1.433	1.432	0.7
graphene	∞	1.431	1.431	0

B. Thermodynamic Stability of Fluorinated Carbon Nanotubes. Hypothetical fluorination of one side of a single graphene sheet results in C_2F-**1** with parallel chains of F atoms. Hence C_2F-**1** can be considered the "planar" C_2F analogue of a graphene sheet. In contrast to the all-carbon case, however, rolling this sheet into an armchair F−SWNT with F atom chains

(36) Dapprich, S.; Komáromi, I.; Byun, K. S.; Morokuma, K.; Frisch, M. J. *J. Mol. Struct. (THEOCHEM)* **1999**, *461*−*462*, 1.
(37) Svensson, M.; Humbel, S.; Froese, R. D. J.; Matsubara, T.; Sieber, S.; Morokuma, K. *J. Phys. Chem.* **1996**, *100*, 19357.
(38) Bauschlicher, C. W. *Chem. Phys. Lett.* **2000**, *322*, 237.
(39) Perdew, J. P.; Burke, K.; Ernzerhof, M. *Phys. Rev. Lett.* **1996**, *77*, 3865.
(40) Perdew, J. P.; Burke, K.; Ernzerhof, M. *Phys. Rev. Lett.* **1997**, *78*, 1396(E).
(41) Becke, A. D. *J. Chem. Phys.* **1993**, *98*, 5648.
(42) Lee, C.; Yang, W.; Parr, R. G. *Phys. Rev. B* **1988**, *37*, 785.
(43) Kudin, K. N.; Scuseria, G. E. *Phys. Rev. B* **2000**, *61*, 16440.
(44) Kudin, K. N.; Scuseria, G. E. *Chem. Phys. Lett.* **1998**, *283*, 61.
(45) Kudin, K. N.; Scuseria, G. E. *J. Chem. Phys.* **1999**, *111*, 2351.
(46) Kudin, K. N.; Scuseria, G. E. *Phys. Rev. B* **2000**, *61*, 5141.
(47) Kudin, K. N.; Scuseria, G. E.; Schlegel, H. B. *J. Chem. Phys.* **2001**, *114*, 2919.
(48) Frisch, M. J.; Trucks, G. W.; Schlegel, H. B.; Scuseria, G. E.; Robb, M. A.; Cheeseman, J. R.; Zakrzewski, V. G.; Montgomery, J. A.; Stratmann, R. E.; Burant, J. C.; Dapprich, S.; Millam, J. M.; Daniels, A. D.; Kudin, K. N.; Strain, M. C.; Farkas, O.; Tomasi, J.; Barone, V.; Mennucci, B.; Cossi, M.; Adamo, C.; Jaramillo, J.; Cammi, R.; Pomelli, C.; Ochterski, J.; Petersson, G. A.; Ayala, P. Y.; Morokuma, K.; Malick, D. K.; Rabuck, A. D.; Raghavachari, K.; Foresman, J. B.; Ortiz, J. V.; Cui, Q.; Baboul, A. G.; Clifford, S.; Cioslowski, J.; Stefanov, B. B.; Liu, G.; Liashenko, A.; Piskorz, P.; Komaromi, I.; Gomperts, R.; Martin, R. L.; Fox, D. J.; Keith, T.; Al-Laham, M. A.; Peng, C. Y.; Nanayakkara, A.; Challacombe, M.; Gill, P. M. W.; Johnson, B.; Chen, W.; Wong, M. W.; Andres, J. L.; Gonzalez, C.; Head-Gordon, M.; Replogle, E. S.; Pople, J. A. *Gaussian 99*, development version (revision B.08+); Gaussian, Inc.: Pittsburgh, PA, 2000.

Chart 2. Orientation of C−C Bonds R1 and R2 with Respect to the Tube Axis

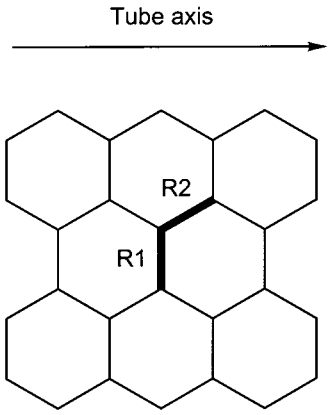

parallel to the tube axis does increase the stability of the system with decreasing tube diameter.[49]

Several geometrical parameters in C_2F-**1** indicate strain, which can be relieved by rolling the sheet into a tube (Figures 2 and 3). The nonbonding distance between fluorine atoms of neighboring chains is only 2.389 Å in C_2F-**1**. Since the fluorine van der Waals radius is 1.35 Å,[50] this close proximity of fluorine atoms causes repulsive interactions. These can be avoided by rolling the C_2F-**1** sheet: the nonbonding distance between fluorine atoms in neighboring chains increases monotonically from 3.076 Å in (12,12) to 5.079 Å in the (3,3) F−SWNT's (Table 2). As was shown for F−SWNT's where the distance between neighboring fluorine rows is sufficiently large to avoid repulsive interactions between rows, the strain is mostly localized within individual zigzag rows of fluorinated carbon atoms.[49] Also, the carbon atoms forming the π bond chains are significantly pyramidalized in C_2F-**1**. The pyramidalization of alkenes has been studied extensively,[51,52] and it is well-known that this deformation can induce significant amounts of strain.[53,54] The symmetric pyramidalization encountered in C_2F-**1** can be characterized by an angle χ defined as the dihedral angle $\angle$C(F)−C=C−C(F).[55] We obtain $\chi = 111.5°$ in C_2F-**1** rather than the regular 180°. The dihedral angle χ is significantly larger in tubular C_2F forms, which approach more planar π systems as the tubes get smaller. Thus, the reduced pyramidalization of the π system is also expected to account for the increased stability of small-diameter F−SWNT's. The dihedral angle χ is −174.3° in (3,3) F−SWNT, indicating that the π systems are slightly pyramidalized away from the tube center. With decreasing tube diameters, the distances between the faces of the π systems of the F−SWNT's decrease, and this is expected to induce repulsive interactions between the π systems. Thus, the tube stability does not increase linearly with D^{-2} but is proportional to D for large diameter tubes.[49]

Similar to our earlier results for (10,10) F−SWNT,[33] we find that all isomers (n,n)-**2** with linear π bond chains studied here are metallic. The C−C bonds of the π bond chains parallel to the tube axis have nonalternating C−C bond lengths, R_{CC}, which decrease from 1.434 Å in C_2F-**1** to 1.419 Å in (3,3) F−SWNT.

To derive thermodynamic properties of F−SWNT's and mean C−F bond dissociation energies (BDE's), we employed isodesmic equations and known heats of formation $\Delta_fH°_{298K}$. But instead of computing the standard reaction enthalpy at 298 K, $\Delta_RH°_{298K}$, for the isodesmic equations under consideration, we restrict ourselves to the classical (i.e., not zero-point-corrected) reaction energy at 0 K since the computation of the necessary vibrational frequencies under periodic boundary conditions is beyond our current possibilities for systems of the size considered here. We anticipate that due to the use of isodesmic equations zero-point vibrational energy and temperature effects should cancel. To test the reliability of our approach, we studied $C_{60}F_{36}$ as Papina et al.[56] recently reported experimental heats of formation and bond dissociation enthalpies for this system. We chose eq 1 to derive the difference in the $C_{60}F_{36}$ and C_{60} heats of formation by using $\Delta_fH°$ of ethene (+12.5399 kcal mol^{-1})[57] and 1,2-difluoroethane (−102.7 kcal mol^{-1}). Note that the latter $\Delta_fH°(CH_2FCH_2F)$ has recently been derived from experimental and theoretical data.[58]

$$C_{60} + 18CH_2F-CH_2F \rightarrow C_{60}F_{36} + 18CH_2{=}CH_2 \quad (1)$$

Then, with the experimental $\Delta_fH°$ of the fluorine atom (+18.97 kcal mol^{-1}),[57] the mean C−F BDE can be calculated according to

$$C_{60}F_{36} \rightarrow C_{60} + 36F \quad (2)$$

The BDE of 74.8 kcal mol^{-1} obtained at the PBE/3-21G level is in reasonable agreement with the experimental estimate of 70.5 ± 0.2 kcal mol^{-1}.[56] The agreement with experiment is significantly improved with PBE/6-31G*//PBE/3-21G single point calculations, since a BDE of 69.3 kcal mol^{-1} is obtained at this level of theory.

An analogous approach uses eqs 3−5 for C_2F systems

$$(C_2)_x + (x/2)CH_2F-CH_2F \rightarrow (C_2F)_x + (x/2)CH_2{=}CH_2 \quad (3)$$

$$(C_2F)_x \rightarrow (C_2)_x + xF \quad (4)$$

$$(C_2)_x + (x/2)F_2 \rightarrow (C_2F)_x \quad (5)$$

and also eqs 6−8 for systems of CF stoichiometry. The latter are investigated in order to compare the fluorination of carbon nanotubes with that of graphite.

$$(C)_x + (x/2)CH_2F-CH_2F \rightarrow (CF)_x + (x/2)CH_2{=}CH_2 \quad (6)$$

$$(CF)_x \rightarrow (C)_x + xF \quad (7)$$

$$(C)_x + (x/2)F_2 \rightarrow (CF)_x \quad (8)$$

The fluorination of natural graphite at high temperature yields gray-white poly(carbon monofluoride), $(CF)_n$, which is comprised of six-membered rings in a chairlike conformation.[59] We model this system by studying a single graphene sheet and a single $(CF)_n$ sheet with the six-membered rings in the chair conformation.

Note that eqs 5 and 8 define the heat of formation of C_2F and CF systems, respectively (Table 3). As we limit ourselves to single graphene sheets or single carbon nanotubes, our

(49) Kudin, K. N.; Yakobson, B. I.; Scuseria, G. E. *Phys. Rev. B* **2001**, *64*, 235−406.
(50) Pauling, L. *The Nature of the Chemical Bond*, 3rd ed.; Cornell University Press: Ithaca, NY, 1960.
(51) Szeimies, G. In *Reactive Intermediates*; Abramovitch, R. A., Ed.; Plenum Press: New York, 1983; Vol. 3, p 299.
(52) Borden, W. T. *Chem. Rev.* **1989**, *89*, 1095.
(53) Meier, W. F.; Schleyer, P. v. R. *J. Am. Chem. Soc.* **1981**, *103*, 1891.
(54) Hrovat, D. A.; Borden, W. T. *J. Am. Chem. Soc.* **1988**, *110*, 4710.
(55) Wijsman, G. W.; Iglesias, G. A.; Beekman, M. C.; de Wolf, W. H.; Bickelhaupt, F.; Kooijman, H.; Spek, A. L. *J. Org. Chem.* **2001**, *66*, 1216.
(56) Papina, T. S.; Kolesov, V. P.; Lukyanova, V. A.; Boltalina, O. V.; Lukonin, A. Y.; Sidorov, L. N. *J. Phys. Chem. B* **2000**, *104*, 5403.
(57) Chase, M. W., Jr. *J. Phys. Chem. Ref. Data, Monogr. 9* **1998**, 1.
(58) Yamada, T.; Bozzelli, J. W. *J. Phys. Chem. A* **1999**, *103*, 7373.
(59) Watanabe, N.; Nakajima, T.; Touhara, H. *Graphite Fluorides*; Elsevier: Amsterdam, 1988.

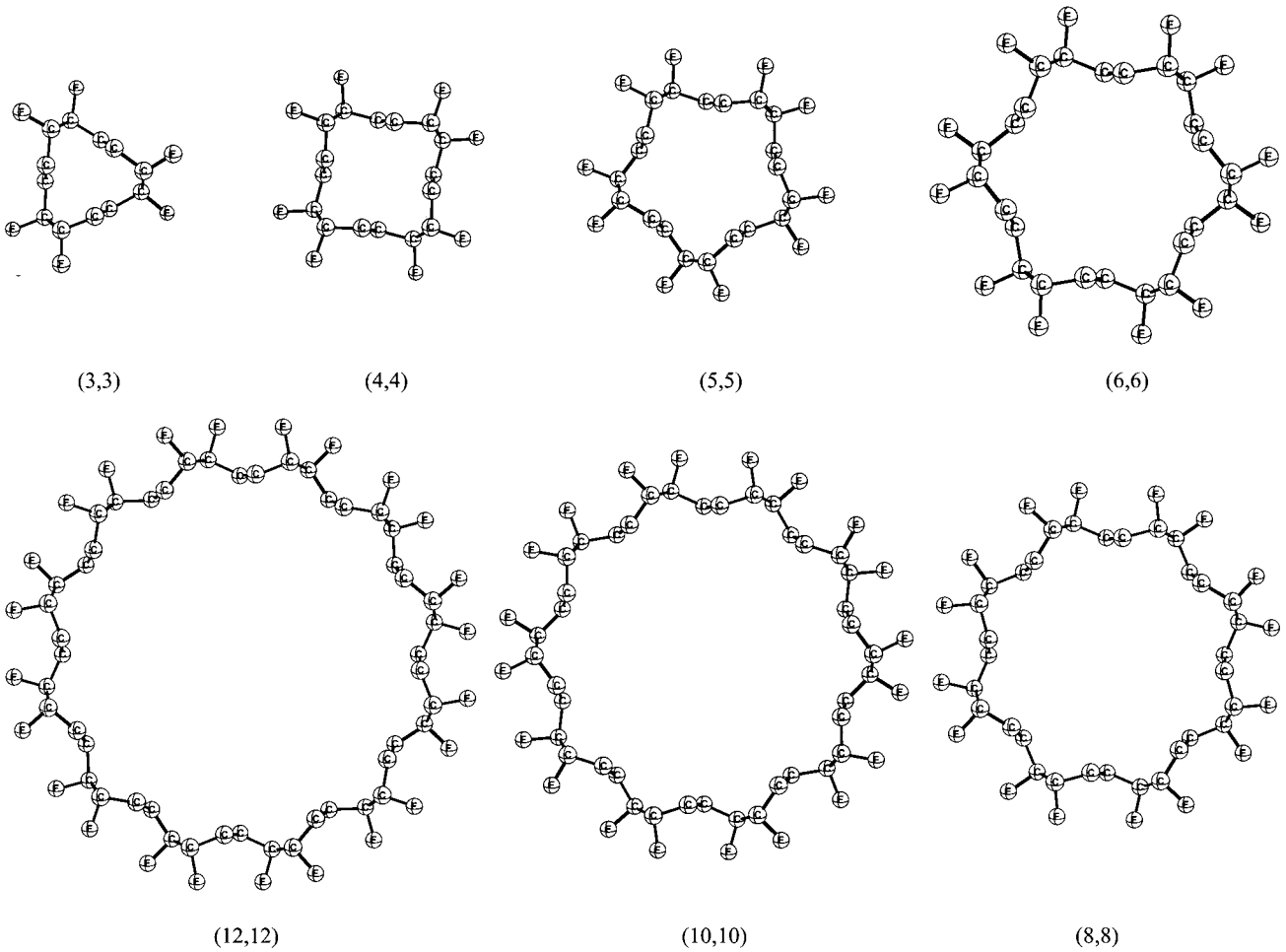

Figure 2. Geometries of fluorinated armchair single wall carbon nanotubes of C_2F stoichiometry, (*n*,*n*)-**2**, viewed along the tube axes as computed at the PBC−PBE/3-21G level of theory.

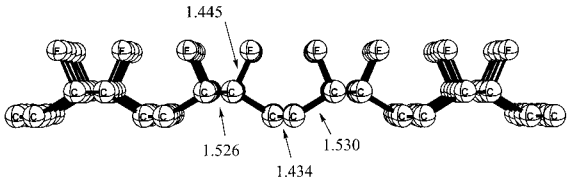

C_2F-**1**

Figure 3. Part of the structure of the C_2F-**1** sheet as computed at the PBC−PBE/3-21G level of theory. Bond lengths are given in angstroms.

approach neglects van der Waals interactions between sheets or tubes. But since these interactions are very weak on a per atom basis, the error introduced by neglecting them is expected to be small compared to the inherent errors of the theoretical method. Indeed, our PBC−PBE/3-21G computations in conjunction with the isodesmic eq 6 gives $\Delta_f H° = -49.2$ kcal mol^{-1} for $(CF)_n$ in very good agreement with the experimental result of -46.7 ± 1.0 kcal mol^{-1}.[60] For the C_2F-**1** sheet, we arrive at $\Delta_f H° = -25.3$ kcal mol^{-1}. Wood et al. fitted the experimental heats of formation of known CF_n compounds and obtained $\Delta_f H°(CF_n) = -(44n + 3n^2)$ kcal mol^{-1};[60] for $n = 1/2$, a $\Delta_f H° = -22.8$ kcal mol^{-1} is expected, in good agreement with our -25.3 kcal mol^{-1} (PBC−PBE/3-21G) value.

The mean C−F bond dissociation energy is smallest for the planar $(C_2F)_n$-**1** sheet and increases with decreasing tube diameter *D* (Figure 4). This change in BDE is due to two synergistic factors (Chart 3): smaller SWNT's are more strained, whereas smaller F−SWNT's are less strained than their larger congeners. Thus, the reactant in eq 4 is stabilized, while the product is destabilized as the tube diameter decreases resulting in the much larger mean BDE's obtained for the smaller F−SWNT's.

We discussed the mean "BDE" above as defined by eqs 2, 4, and 7. However, the term "bond energy" is also in use in the chemical literature. We follow Pauling and distinguish here between these two terms: the *bond energy* is defined in such a

Table 2. The Carbon−Carbon Distance (R_{CC}, Å) in the Nonalternating π Bond Chains, the C−F Bond Lengths [*r*(C−F), Å], the Nonbonding Fluorine−Fluorine Distance (Å) between neighboring rows, the Dihedral Angle [∠C(F)−C═C−C(F), deg], and the Strain Energy (E_s, kcal mol^{-1}) of Fluorinated (*n*,*n*) Single Wall Nanotubes per C_2F Group Obtained at the PBC−PBE/3-21G Level of Theory[a]

n	R_{CC}/Å	*r*(C−F)/Å	*d*(F−F)/Å	∠C(F)−C═C−C(F)/deg	E_s/(kcal mol^{-1})
3	1.419	1.411	5.079	−174.3	−18.2
4	1.419	1.419	4.448	164.6	−18.3
5	1.420	1.424	4.050	153.1	−16.7
6	1.421	1.428	3.785	145.9	−15.0
8	1.423	1.432	3.440	136.8	−12.2
10	1.424	1.435	3.224	131.1	−10.2
12	1.425	1.437	3.076	127.1	−8.8
C_2F-**1**	1.434	1.445	2.389	111.3	0

[a] A negative E_s indicates that the tubular form is more stable than the "planar" C_2F-**1**.

(60) Wood, J. L.; Badachhape, R. B.; Lagow, R. J.; Margrave, J. L. *J. Phys. Chem.* **1969**, *73*, 3139.

Table 3. Bond Dissociation Enthalpy (BDE, kcal mol^{-1}) per Fluorine Atom and the Heats of Formation ($\Delta_f H°$, kcal mol^{-1}) of C_2F Single Wall Carbon Nanotubes Determined at the PBC−PBE/3-21G Level of Theory

structue	BDE/(C−F bond)/ (kcal mol^{-1})	$\Delta_f H°$/(kcal mol^{-1})
(3,3)	83.1	−43.5
(4,4)	74.4	−43.6
(5,5)	68.6	−42.0
(6,6)	64.6	−40.3
(8,8)	59.5	−37.5
(10,10)	56.5	−35.6
(12,12)	54.4	−34.1
$(C_2F)_n$-**1**[a]	44.3	−25.3
$C_{60}F_{36}$	74.8 (expt: 70.5 ± 0.2)[56]	
$(CF)_n$	68.2	−49.2 (expt: −46.7 ± 1.0)[60]

[a] Note that this does not correspond to the structure obtained experimentally but to the hypothetical structure depicted in Chart 1 and Figure 3.

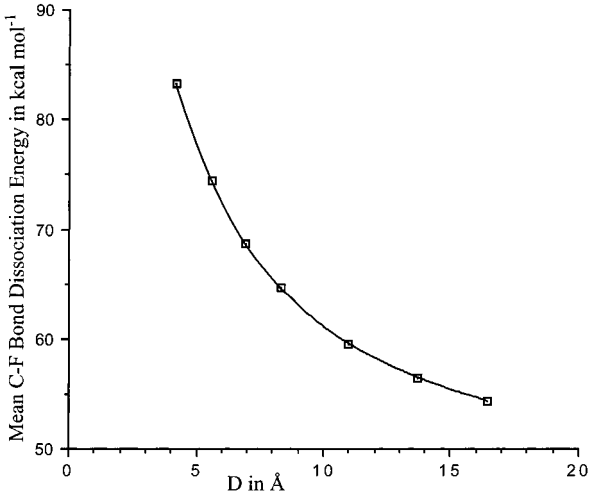

Figure 4. Mean C−F bond dissociation energies (kcal mol^{-1}) in fluorinated single wall carbon nanotubes. Data obtained at the PBC−PBE/3-21G level of theory.

Chart 3. Comparison of Average C−F Bond Dissociation Energies for SWNT's and F−SWNT's[a]

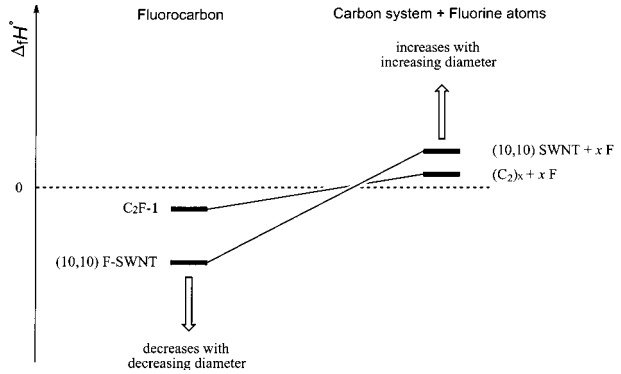

[a] As the stability of the F−SWNT's increases (their energy decreases) with decreasing diameter and as the stability of bare SWNT's decreases (their energy increases) at the same time, the average C−F bond dissociation energy (BDE) is larger for small-diameter nanotubes.

way "that the sum over all bonds of a molecule which can be satisfactorily represented by a single valence-bond structure is equal to the enthalpy of formation of the molecule from its constituent atoms in the normal states."[50] The C−F bond energy in $(CF)_n$ was derived by Wood et al. to be around 115 kcal mol^{-1}.[60] The mean BDE, however, is only 66 kcal mol^{-1} according to our computational analysis. Although the C−F bond is very weak in C_2F-**1**, its strength in the (5,5) F−SWNT is similar to that of $(CF)_n$ or to that in $C_{60}F_{36}$.[56]

According to eq 5, the fluorination of thinner SWNT's is significantly more exothermic than that of wider tubes. This suggests that thin tubes can be fluorinated at lower temperatures. On the other hand, thermal removal of the fluorine cover yielding pristine SWNT's from C_2F fluorinated tubes should require harsher conditions for smaller F−SWNT's.

C. Endohedral F Atoms. In our previous investigation of the fluorinated (10,10) SWNT's, we found that a 5.4 kcal mol^{-1} more stable F-SWNT (10,10)-**3** can be obtained by moving 50% of the fluorine atoms of (10,10)-**2** inside the tube so as to preserve the nonalternating π bond chains.[33] The fluorination inside the tube will not be as favorable for smaller tubes due to the anticipated repulsive fluorine−fluorine interactions. Indeed, we find here that the (5,5)-**3** F−SWNT, the analogue to (10,10)-**3**, is 9.9 kcal mol^{-1} *higher* in energy than the all-outside isomer (5,5)-**2**. The nonbonding F···F distance is only 2.19 Å, whereas the fluorine van der Waals radius is 1.35 Å.[50]

In this context, the question arises if a single fluorine atom, were it able to get inside a narrow SWNT through either open tube ends or side wall holes, is able to bind covalently to the concave surface. Steric repulsion between inside-bound fluorine atoms and the electron clouds of the carbon nanotube π system might be significant. Also, the lobes of π orbitals on the carbon atoms will not have the same size on either side of the nanotube surface due to the curvature of the tube. The latter causes pyramidalization at the carbon atoms which in turn leads to rehybridization of the p_z(C) orbitals as 2s orbital character is mixed into the p_z(C) to some amount.[61] The outer lobe will be larger than the inner one, and thus the orbital overlap, essential for covalent chemical binding, will be reduced for the fluorine atom inside the SWNT.[62] Bulusheva et al. concluded that the inner surface of a nanotube should preferentially bind electron donors, whereas the outer surface should be more reactive toward electron acceptors.[63]

Endohedral binding and the effect of pyramidalization have been studied in the [60]fullerene where the surface is curved in more than one direction. In terms of Haddon's "π-orbital axis vector analysis" (POAV1),[64,65] the different curvatures of the C_{60} and (5,5) SWNT surfaces are reflected by pyramidalization angles of 11.6° and 6.6°, respectively.[66] As the carbon atoms in C_{60} are more pyramidalized than those in a (5,5) SWNT, the above considerations suggest that endohedral covalent binding to the concave surface should be more disfavored for C_{60} than for SWNT's of similar diameter. Indeed, in the remarkable endohedral fullerene N@C_{60}, the nitrogen atom is in its atomic ground state and is not bound to the carbon cage.[62,67−72] This complex is stable enough to allow typical C_{60} chemistry on its exohedral surface while the endohedral surface is not attacked by the nitrogen atom even after extended stirring at ambient temperatures.[69,71] Mauser et al.[62] have demonstrated in a thoughtful computational study using a combination of UB3LYP hybrid density functional theory and the semiempirical (PM3) Hamiltonian that the N@C_{60} complex with the N($^4S_{3/2}$) atom in the

(61) Haddon, R. C. *Acc. Chem. Res.* **1992**, *25*, 127.
(62) Mauser, H.; van Eikema Hommes, N. J. R.; Clark, T.; Hisch, A.; Pietzak, B.; Weidinger, A.; Dunsch, L. *Angew. Chem.* **1997**, *109*, 2858; *Angew. Chem., Int. Ed. Engl.* **1997**, *36*, 2835.
(63) Bulusheva, L. G.; Okotrub, A. V.; Romanov, D. A.; Tomanek, D. *J. Phys. Chem. A* **1998**, *102*, 975.
(64) Haddon, R. C. *Acc. Chem. Res.* **1988**, *21*, 243.
(65) Haddon, R. C. *J. Am. Chem. Soc.* **1990**, *112*, 3385.
(66) Haddon, R. C.; Brus, L. E.; Raghavachari, K. *Chem. Phys. Lett.* **1986**, *131*, 165.

cage center is slightly more stable than separated N($^4S_{3/2}$) and C_{60} by 1 kcal mol^{-1}.[62] These authors also showed that binding of the N atom to the carbon atoms of the concave C_{60} surface is 82−84 kcal mol^{-1} less favorable than exohedral binding and 34 kcal mol^{-1} less favorable than an unbound free nitrogen atom in the center of the C_{60} cage. Although F@C_{60} has been studied computationally,[70] the binding of the fluorine atom to the concave surface has not been probed. We therefore decided to study the C_{60}F system as a prototype for comparison with exo- and endohedral binding of fluorine atoms to SWNT sidewalls.

With the 3-21G basis set and the PBE functional the endohedral binding of the F atom to the concave surface is exothermic with respect to separated C_{60} ($\tilde{X}^1A_g$) and F(^{2}P) species. The C−F bond length is found to be 1.607 Å at the PBE/3-21G level. At the B3LYP/3-21G level, the endohedral binding is almost thermoneutral; the C−F bond length (1.609 Å) is similar to the PBE/3-21G value. But as the basis set is enlarged to 6-31G* (using either the PBE or B3LYP functionals), the C−F distance increases significantly to 2.60 Å so that the fluorine atom symmetrically bridges the 6,6 bond of the fullerene. The structure is stabilized by 23.0 and 13.4 kcal mol^{-1} (PBE and B3LYP, respectively) relative to the separated species due to a partial charge transfer from the C_{60} cage to the fluorine atom. These results indicate that the smaller 3-21G basis set is not flexible enough to describe the repulsive interactions between the fluorine lone pairs and the concave C_{60} surface. In addition, basis set superposition errors are expected to be sizable when modeling the endohedral interaction with the concave C_{60} surface with the small 3-21G basis set.

As expected, the exohedral addition is much more favorable at all levels of theory employed. The PBE functional yields slightly longer C−F bonds than B3LYP, while with the 6-31G* basis the C−F bonds are shorter than with the 3-21G basis set. But note that at PBE the binding energy is approximately 10 kcal mol^{-1} larger than that obtained with B3LYP, irrespective of the basis set employed. To summarize, an endohedral fluorine atom does not bind covalently to a carbon atom but rather is stabilized inside the cage by charge transfer.

A different situation is revealed for endohedral covalent binding of fluorine in a (5,5) single wall carbon nanotube although this tube has a diameter similar to that of the C_{60} molecule. But as the pyramidalization of the carbon atoms in the (5,5) SWNT is smaller than in C_{60} (the SWNT surface is only curved in one direction), endohedral addition is by far more favorable than inside C_{60}. Both exo- and endohedral addition modes are strongly exothermic with respect to separated species (Table 4). The C−F bond length inside the tube is 1.514 Å, whereas it is 1.451 Å outside. Our computations suggest that it seems very likely that a fluorine atom would attack the inner surface of a bare SWNT, even in the case of the small (5,5) tube. With increasing tube diameter the preference of the outside addition should decrease until in the limit of an infinitely wide tube both modes are degenerate.

Endohedral binding of the F atom reduces the width inside the (5,5) tube from 6.9 Å to a maximum of 4.8 Å (Figure 5). Considering fluorine and carbon van der Waals radii of 1.35 and 1.6 Å (about half the intertube distance in CNT ropes[9]), a cavity of only 1.8 Å remains. On the other hand, the (6,6) SWNT (D = 8.3 Å) should have a cavity width of 3.2 Å on the basis of the above parameters, and hence fluorine atom diffusion along the tube axis should be possible even after one F atom is bound to the concave surface.

Table 4. Relative Energies (kcal mol^{-1}) for the Addition of a Single Fluorine Atom to C_{60} and to a (5,5) SWNT Model ($C_{90}H_{20}$) Obtained at Various Levels of Theory

structure	PBE/ 3-21G	PBE/ 6-31G*	B3LYP/ 3-21G	B3LYP/ 6-31G*
C_{60} + F(^{2}P)	0	0	0	0
C_{60}F endohedral	−13.2	−23.0	+1.0	−13.4
C_{60}F exohedral	−61.8	−63.4	−51.3	−55.0
(5,5)-SWNT + F(^{2}P)	0	0		
(5,5)-SWNT-F, ^{2}A′, inside	−40.0	−38.7		
(5,5)-SWNT-F, ^{2}A′, outside	−69.1	−68.5		

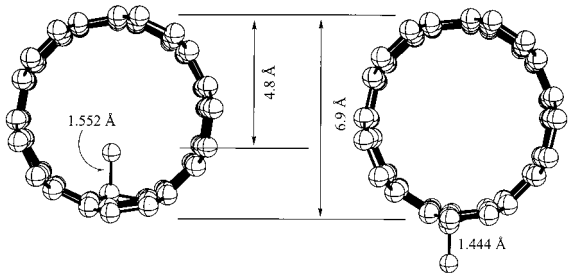

Figure 5. Geometries of exo- and endohedrally fluorinated (5,5) single wall carbon nanotubes ($C_{90}H_{20}$ model) viewed along the tube axes as computed at the PBE/3-21G level of theory.

The addition of a single F atom to the inside or outside of (5,5) SWNT results in a radical C_xF(^{2}A′) with a strong delocalization of the unpaired spin. The preferred site for the addition of a second fluorine atom should not be governed by a particularly high spin density at a given carbon atom but rather by the thermodynamic stability of the resulting C_xF_2 compound.

D. Nature of the C−F Bond. Due to the structural and energetic similarities of SWNT with graphite, a comparison of fluorinated SWNT with well-known graphite−fluorine compounds is instructive. The fluorination of graphite is well understood today and is described in detail in the monograph of Watanabe et al.[59] Below 400 °C $(C_2F)_n$ is formed, whereas as the material obtained above 600 °C consists of $(CF)_n$.[59,73] Between approximately 400 and 600 °C a mixture of the two graphite fluoride forms results. Note that the $(C_2F)_n$ obtained at T < 400 °C tarnishes glass after a few months due to the gradual release of absorbed F_2, but this is not observed with $(CF)_n$ samples. Both graphite fluorides have strongly corrugated carbon sheets with the six-membered rings in chairlike cyclohexane conformations.[59,73,74] Two sheets are linked by covalent C−C bonds in $(C_2F)_n$.[73] The C−F bonds in the graphite fluorides are 1.41 Å long and covalent. We obtain a C−F bond length of 1.401 Å at PBC−PBE/3-21G level of theory in reasonable agreement with experiment. The C−F bonds obtained in our PBC−PBE calculations of C_2F F−SWNT's discussed above and depicted in Figure 2 range from 1.41 to 1.45 Å and are thus slightly longer than in the covalent graphite fluoride $(CF)_n$.

A comparison of the Mulliken charges on the F atoms in fluorotubes and fluorocarbons such as CH_3F, CF_4, poly(fluoroethylene) $(CF_2)_n$, and $(CF)_n$ is instructive. Mulliken charges

(67) Almeida Murphy, T.; Pawlik, T.; Weidinger, A.; Höhne, M.; Alcala, R.; Spaeth, J.-M. *Phys. Rev. Lett.* **1996**, *77*, 1075.
(68) Knapp, C.; Dinse, K.-P.; Pietzak, B.; Waiblinger, M.; Weidinger, A. *Chem. Phys. Lett.* **1997**, *272*, 433.
(69) Pietzak, B.; Waiblinger, M.; Almeida Murphy, T.; Weidinger, A.; Höhne, M.; Dietel, E.; Hirsch, A. *Chem. Phys. Lett.* **1997**, *279*, 259.
(70) Lu, J.; Zhang, X.; Zhao, X. *Chem. Phys. Lett.* **1999**, *312*, 85.
(71) Dietel, E.; Hirsch, A.; Pietzak, B.; Waiblinger, M.; Lips, K.; Weidinger, A.; Gruss, A.; Dinse, K.-P. *J. Am. Chem. Soc.* **1999**, *121*, 2432.
(72) Greer, J. C. *Chem. Phys. Lett.* **2000**, *326*, 567.
(73) Touhara, H.; Kadono, K.; Fujii, Y.; Watanabe, N. *Z. Anorg. Allg. Chem.* **1987**, *544*, 7.
(74) Kita, Y.; Watanabe, N.; Fujii, Y. *J. Am. Chem. Soc.* **1979**, *101*, 3832.

are known to be sensitive to the basis set size; the absolute charges obtained might not be very meaningful, but a comparison among similar systems to reveal trends should nonetheless be possible. We find that the charges on the fluorine atoms in CH_3F ($-0.27e$), CF_4 ($-0.24e$), $(CF_2)_n$ ($-0.22e$), $(CF)_n$ ($-0.18e$), and fluorotubes ($-0.17e$ to $-0.20e$) are similar at the PBE/3-21G level of theory. Note that there is only little dependence on the tube diameter [comparing (10,10) and (5,5) fluorotubes] and on the fluorine decoration [among (10,10) fluorotubes].

Finally, the covalent graphite fluorides $(CF)_n$ and $(C_2F)_n$ show strong IR bands at 1219 and 1221 cm^{-1}, respectively, due to ν(C−F) stretching vibrations.[59] The F−SWNT's produced by fluorination of SWNT's above 250 °C exhibit strong bands in the infrared region between 1220 and 1250 cm^{-1}.[19] Hence, all available data, computed bond lengths and charges, and experimental vibrational spectra indicate that the C−F bonds in the F−SWNT's are similar to those in the so-called "covalent" $(CF)_n$. This conclusion was also reached by Mickelson et al. on the basis of the IR data.[19]

The C−F bonds in F−SWNT's studied here are somewhat longer than in $(CF)_n$. This can be due to the repulsive interaction with the neighboring fluorine atoms in the same row. As pointed out in our previous investigation, the shortest nonbonding F···F distances in all-outside fluorinated (10,10) F−SWNT's (2.36−2.50 Å) are smaller than twice the van der Waals radius (2.70 Å).[33] The C−F bonds are also in close proximity to the conjugated π systems, and hence an additional repulsive interaction exists.

IV. Conclusions

Our PBC−PBE computations indicate that rolling the C_2F-**1** sheet (Chart 1, Figure 3), a graphene sheet fluorinated on one side and having zigzag π bond chains, into a tube reduces the repulsive nonbonding interactions between the fluorine atoms of the C_2F-**1** sheet and the pyramidalization of the C═C double bonds. Small diameter fluorinated single wall carbon nanotubes of C_2F stoichiometry (F−SWNT's) are thermodynamically more favorable than wider ones.[49] This observation is in contrast to a pristine graphene sheet and SWNT's, as the strain of the latter increases with decreasing diameter. As a consequence of the opposing trends in strain contents, the fluorination of SWNT's is more exothermic for narrower tubes. Conversely, the mean C−F bond dissociation energies increase with decreasing tube diameter. The average strength of the C−F bond in the (5,5) F−SWNT's studied here is similar to that in poly(carbon monofluoride) $(CF)_n$. It is expected that monovalent substituents other than fluorine, e.g., the alkyl groups introduced through lithium organyls,[22] have qualitatively the same effect on the thermodynamic stability of the derivatized SWNT's.

Finally, a remark on the fluorination of multiwall carbon nanotubes by Nakajima[23] is worthwhile. Nakajima et al. obtained XPS and IR data from fluorinated multiwall carbon nanotubes (stage 1 C_4F-C_5F obtained between RT and 60 °C) consistent with semicovalent C−F bonds.[23] However, fluorine is only bound to the outer layers of the MWNT's. With increasing fluorination temperatures (300−400 °C) the nature of the C−F bonds becomes more covalent, but TEM images indicate that this is due to the formation of several layers of graphite fluoride $(CF)_n$ on the outer layers of the MWNT's.[23] Also, partial decomposition of the tubes and lower crystallinity was observed possibly due to formation of cracks in the MWNT's. The MNWT's used by Nakajima et al. had an average outer diameter of 18.4 nm and consisted on the average of 22 rolled graphene layers.[23] Since these tubes are about an order of magnitude wider than the tubes fluorinated by Mickelson et al., the completely different properties of the obtained fluorinated tubes come as no surprise in view of our computations. The formation of C_2F structures with conjugated π bond chains is thermodynamically much less favorable for very wide CNT's. In addition, endohedral fluorination is expected to be less unfavorable than in narrow tubes and hence the complete fluorination [i.e., formation of $(CF)_n$] of a few outside layers of the tube is conceivable.

Acknowledgment. This work was supported by the National Science Foundation (NSF), Grant No. CHE-99825165. We thank Professors Dr. R. H. Hauge, Dr. J. L. Margrave, and Dr. R. E. Smalley for inspiring discussions.

Note Added in Proof: The side wall functionalization of single wall carbon nanotubes has recently been reported by Bahr et al. (*J. Am. Chem. Soc.* **2001**, *123*, 6536) and Holzinger et al. (*Angew. Chem.* **2001**, *113*, 4132; *Angew. Chem., Int. Ed. Engl.* **2001**, *40*, 4002).

Supporting Information Available: Cartesian coordinates and absolute energies of all stationary points (PDF). This material is available free of charge via the Internet at http://pubs.acs.org.

JA010977J